Nonlocal complex potential theory of dissociative electron attachment: Inclusion of two vibrational modes

H. B. Ambalampitiya and I. I. Fabrikant

Department of Physics and Astronomy,

University of Nebraska, Lincoln, Nebraska 68588-0111, USA

(Dated: March 2, 2020)

Abstract

The cross section of dissociative electron attachment (DEA) to polyatomic molecules strongly depends on the number of vibrational modes in the target molecule. In the present paper, we develop the nonlocal complex potential theory to treat the disscoiation dynamics when there are more than one vibrational mode in the neutral molecule. We also introduce a semiclassical approach to obtain cross section by computing the matrix elements of the Green's function and the electron capture amplitudes using classical trajectories. We demonstrate the application of the multimode nonlocal and semiclassical theories to a generic molecule of type CY_3X with the inclusion of symmetric C−X stretch and CY_3 deform (" umbrella") vibrational modes . Finally we present and compare the DEA cross section for CF_3Cl computed using both nonlocal and semiclassical approaches.

PACS numbers:

I. INTRODUCTION

Dissociative electron attachment (DEA) to molecules is an important process in gaseous dielectrics and other environments including excimer lasers, discharges used for etching, the earth's atmosphere, astrophysics, and radiation damage [1–4]. The complexity in the interaction between the electron and nuclear motions during a DEA process is what makes the theoretical description of DEA challenging. Earlier theoretical studies on DEA have mainly focused on simpler molecules such as diatomics [5–7] where the nuclear motion in the resonant state is purely one dimensional. A lot of efforts has recently been made to include several vibrational degrees of freedom in DEA [8–15]. All this work has been done in the framework of the local approximation, or the boomerang model [16]. In this model, the motion of the intermediate negative-ion state is described by a Schrödinger equation with a local complex potential whose imaginary part is responsible for the electron autodetachment. However, the exact potential describing this motion is in fact a nonlocal energy dependent operator [17–20]. Nonlocal effects are important when the width of the negative ion resonance is large, for example in low-energy DEA to H_2 molecule [20]. They are also crucial in description of threshold structures and vibrational Feshbach resonances [21].

In view of the tremendous amount of computational work necessary to obtain multidimensional complex potential energy surfaces and the solution of the multidimensional Schrödinger equation for the nuclear motion, it is apparent that the way to solve DEA problems for molecules larger than triatomic is to make further (in addition to local) approximations. One approach is to "freeze" all vibrational modes other than that which is most important for the DEA process. Sometimes this dominant mode can be associated with the reaction coordinate, and then one-dimensional model for vibrational dynamics can be justified. However, in many cases this mode cannot be identified, and inclusion of several vibrational modes becomes essential. Typical examples are DEA to CO_2 [22] and water [12, 13] molecules. In other cases, although the mode dominant in DEA process can be identified, the influence of other modes on the DEA dynamics is important. We will consider a process of the type

$$e + AB(\nu) \to AB^- \to A(\mu) + B^-$$

where ν is the set of vibrational quantum numbers identifying the initial state of the molecule AB and μ is a set of vibrational quantum numbers identifying the final state of the fragment

A. We assume that the anion fragment B^- is atomic.

Typical examples are methyl halides and perfluoromethyl halides. The process

$$e + CY_3X \rightarrow CY_3X^- \rightarrow CY_3 + X^-. \quad (1)$$

where X stands for a halogen atom, and Y for the H or F atom, can be reasonably described by a model with one active coordinate corresponding to C-X stretch vibration [23–25]. However, it was shown [14, 15] that in the CF_3Cl case the symmetric deformation vibrations can strongly influence the dissociation dynamics. This was found by performing local DEA and vibrational excitation calculations for the process

$$e + CF_3Cl(\nu_2, \nu_3) \rightarrow CF_3Cl^- \rightarrow CF_3(\nu_2') + Cl^-,$$

Here ν_2, ν_3 stand for symmetric deformation vibrations (or so-called "umbrella" mode) and symmetric stretch C-Cl vibrations. Only one mode, in addition to the reaction mode ν_3, was included.

The molecule CF_3Cl belongs to the C_{3v} point group. The low-energy shape resonance driving the DEA process at $E = 1.8$ eV has the A_1 symmetry. Therefore, the degenerate vibrations of the E symmetry, CF d-stretch (ν_4), CF_3 d-deform (ν_5) and CF_3 rock (ν_6) [27] can be excited resonantly only in pairs. Conversely, if the molecule is initially in vibrationally excited state of the E symmetry, the direct electron capture into the resonant state of the A_1 symmetry is not possible. (It is possible only as a second-order process). We can also assume that the symmetric CF stretch vibration (ν_1) is unlikely to be excited as the C-F bond length in CF_3Cl, 1.34 Å[28] is very close to that of the anion (1.37 Å[28]) and the free radical CF_3 (1.32 Å[29]). Accordingly we can assume that initial excitation of the symmetric C-F stretch does not influence substantially the DEA process. These assumptions are also justified by experimental results [30] showing a strong electron-impact vibrational excitation of ν_2 and ν_3 modes via the low-energy A_1 resonance while the other vibrational modes were not significantly excited.

Inclusion of additional vibrational modes in the theoretical description of DEA to molecules of type CY_3X is of interest due to two major reasons. First, the inclusion of ν_2 mode in DEA calculations of DEA to CY_3X provides the internal energy of the CY_3 radical. This energy can be affected by the interaction of final-state products: CY_3 and X^- or due to a significant Frank-Condon factor for transition between the initial CY_3X state

and the antibonding CY_3X^- state. Previous studies of low-energy electron attachment to CH_3I, CF_3I and CF_3Br [31] have shown an insignificant internal energy redistribution in the final products whereas for high-energy electrons, final state interaction becomes important [32–34]. The second reason to include additional vibrational modes in DEA is the strong sensitivity of DEA cross section to the initial vibrational state of the target molecule. Previous DEA calculations done with one-mode approximation for methyl halides [24, 25, 35, 36] have explained well the observed temperature dependence of DEA cross section for these compounds. However, situation is somewhat different with perfluoromethyl halides. The one-mode approximation for CF_3Cl [23, 37] could not confirm the observed low-energy peak in the DEA cross section at the vibrational temperature $T = 800$ K [38]: the calculated peak is too narrow as compared to the experiment. It looks like the theoretical cross section at low electron energies is not growing fast enough with the vibrational energy. For the CF_3Br the same pattern was noticed [39]: the rate of dissociative attachment calculated with one-mode approximation results in a slower growth at high vibrational temperatures as compared to the experimental observations. This suggests that the excited vibrational modes in perfluoromethyl halides are important, perhaps because at a given vibrational temperature they are more populated than in methyl halides. Since these strong vibrational temperature effects occur at low electron energies, where the local approximation fails, the nonlocal theory is needed to describe these peaks.

The goal of the present paper is to give a general formulation of the nonlocal DEA theory for molecules with more than one vibrational degrees of freedom and demonstrate this theory for a model molecule of the type CY_3X with inclusion of two vibrational degrees of freedom. In the present paper we concentrate on the nuclear dynamics, and are not concerned with accurate calculation of complex potential energy surfaces. To illustrate our method, we use previous calculation of the surfaces for CF_3Cl which are parametrized in an analytical form convenient for calculations.

We will explore completely quantum version and semiclassical version of the theory. Completely quantum nonlocal calculations become infeasible when the number of degrees of freedom exceeds three, therefore the classical or semiclassical treatment of nuclear motion should be explored. At this point we specify what we mean by classical, semiclassical and quasiclassical approaches. First, in all three methods the electron motion is treated quantum-mechanically, and we distinguish different methods by the way the nuclear motion

is treated. The classical approach [14, 40–42] was developed within the framework of the local theory, and it is not clear how to extend it to the nonlocal version, mainly because there is no classical analogue of the nonlocal complex potential. The quasiclassical approach [43, 51] starts with the Schrödinger equation for the nuclear motion, and finds its solution in the WKB approximation modified by the uniform Airy function approximation. All integrals involving calculation of capture amplitudes and matrix elements of the Green's function are calculated by the stationary phase method corresponding to the Franck-Condon principle. Quasiclassical calculations of DEA to many molecules were done in the past. However, generalization of this method to multidimensional case presents big challenges, therefore at this point we switch to the semiclassical methods based on the Van-Vleck-Gutzwiller propagator. A general formulation of quantum and semiclassical theories will be given in Secs. We apply then the general formulation to DEA to the CF_3Cl molecule in Sec. . Results are presented in Sec.

II. COORDINATES AND HAMILTONIAN

We start with a general case describing a polyatomic molecule with N vibrational degrees of freedom, but, as we go along, we will be introducing several approximations appropriate to DEA to a generic CY_3X molecule.

We use first the Born-Oppenheimer approximation allowing us to describe molecular motion in terms of the potential energy surface U^0. In addition we assume a fixed orientation of the molecule in the initial state, so that the Hamiltonian of the system in the initial state can be written as

$$H_i = H_M(p_1, ..., p_N, q_1, ..., q_N) + H_e(\mathbf{r}, q_1, ..., q_N)$$

where $q_1, ..., q_N$ are internal vibrational coordinates for the neutral molecule, $p_1, ..., p_N$ are conjugated momenta, and $\mathbf{r}$ is the electron position vector. The electron Hamiltonian H_e can be written as

$$H_e = T_e + V(\mathbf{r}, q_1, ..., q_N)$$

where T_e is the electron kinetic energy, and $V(\mathbf{r}, q_1, ..., q_N)$ is the electron interaction with the molecule. We assume one-electron approximation by incorporating effectively all interactions, including exchange and correlation, into V. The Hamiltonian of the molecule H_M

is

$$H_M = T_M(p_1, ...p_N) + U^0(q_1, ..., q_N)$$

where U^0 is the potential energy surface for the ground electronic state. The eigenvalues of the operator H_M are ϵ_ν where $\nu = \{\nu_1, ..., \nu_N\}$ is the set of vibrational quantum numbers for the neutral molecule.

The final-state Hamiltonian is represented in the form

$$H_I = T(P_r, P_1, ..., P_{N-1}; Q_r, Q_1, ..., Q_{N-1}) + U^-(Q_r, Q_1, ..., Q_{N-1}) \tag{2}$$

where $Q_1, ..., Q_{N-1}$ are vibrational coordinates of the products, and $P_1, ..., P_{N-1}$, are corresponding conjugated momenta, Q_r, P_r are the reaction coordinate and conjugated momentum, and U^- is the anion complex potential as a function of coordinates Q. We assume that at $Q_r \to \infty$ H_I can be separated as

$$H_I = T_{\rm rel}(P_r, Q_r) + T_p(P_1, ..., P_{N-1}; Q_1, ..., Q_{N-1}) + U^-(\infty, Q_1, ...Q_{N-1})$$

where $T_{\rm rel}$ is the kinetic energy of the relative motion, and T_p kinetic energy of the products.

Generally rotational coordinates should be included as well, because the internuclear axis can start rotating as a result of dissociation. However, assuming a symmetric dissociation of the type relevant to reaction (1), we neglect the rotational effects.

III. RESONANT R-MATRIX THEORY

Resonant R-matrix theory of DEA [43] is completely equivalent to the nonlocal complex potential theory, and was used before [23] for calculation of DEA to CF_3Cl in one-mode approximation. Since this version is convenient for model calculations, we will extend it to the multimode version.

Employing the Born-Oppenheimer approximation, we start by writing the Schrödinger equation for the electron motion with fixed nuclear coordinates

$$H_e\Psi = E_e\Psi$$

where E_e is the electron energy. In one-electron approximation the solution Ψ, after its expansion in spherical harmonics, can be represented by the $L_{\max} \times L_{\max}$ matrix $\psi_{lml'm'}(r, q_1, ..., q_N)$ where $L_{\max}$ is the maximum number of angular momentum channels

lm included in the expansion of the wavefunction for a given symmetry of the negative-ion resonance. We then introduce the R-matrix sphere of radius r_0 outside which only long-range interactions are important. The R matrix can be written as

$$R(q) = \psi \left(\frac{d\psi}{dr} \right)^{-1} \Bigg|_{r=r_0}$$

where q represents the totality of all vibrational coordinates of the target $q_1, ..., q_N$.

Turning now to the resonant theory, we assume for simplicity that only one angular mode dominates the resonant scattering, so that the R matrix is reduced to one element, R-function $R(q)$. This is a typical assumption used in most DEA calculations. However, for calculation of the angular distribution of the products the theory should be developed further to include several angular modes [44, 45].

In the resonant approximation we keep one pole term of the R-matrix expansion plus a background term R_b independent of q [43]

$$R(q) = \frac{\gamma^2(q)}{E_1(q) - E_e} + R_b(E_e).$$

where $\gamma(q)$ is the R-matrix surface amplitude, $E_1(q)$ is the first pole corresponding to the negative-ion resonance, and E_e is the electron energy. To include vibrational motion we replace $E_1(q)$ by the Hamiltonian for the anion motion [43, 46], so that the R function becomes an operator

$$R(q) = \gamma(q)[H_I - E]^{-1}\gamma(q) + R_b(E) \tag{3}$$

where E is the total energy of the system, including the vibrational energy, and H_I is the negative-ion Hamiltonian. To incorporate the outgoing-wave boundary conditions in the dissociating channel we add to energy E in Eq. (3) an infinitesimal $i\eta$ and represent the Hamiltonian H_I in the final-state form given by Eq. (2).

Next we solve the equation for the S operator by substituting Eq. (3) into the basic equation of the R-matrix theory and using the representation of vibrational eigenstates of the neutral molecule

$$u = R \left. \frac{du}{dr} \right|_{r=r_0} \tag{4}$$

where u is the matrix of electron radial wavefunctions at $r > r_0$

$$u = u^- - u^+ S$$

where $u^{\pm}$ are matrices with the asymptotic form

$$u^{\pm}_{\nu\nu'} \sim k_\nu^{-1/2} e^{\pm i k_\nu r} \delta_{\nu\nu'}$$

where k_ν are electron wavenumbers in corresponding vibrational channels, $k_\nu^2 = 2(E - \epsilon_\nu)$, ϵ_ν are energy eigenstates for the neutral molecule. In accordance with the one-angular-mode approximation, we will assume from now on that u, $u^{\pm}$, and S are diagonal in lm, and R in Eq. (3) has only one nonzero matrix element for $l = l_r$, $m = m_r$ where l_r, m_r are angular momentum and its projection dominating the resonance scattering.

Solving Eq. (3) leads to the following representation for the S operator [47, 48]

$$S = \frac{\tilde{u}^-}{\tilde{u}^+} - \frac{2i}{\tilde{u}^+}\gamma(E - H_I - F)^{-1}\gamma\frac{1}{\tilde{u}^+} \tag{5}$$

where

$$\tilde{u}^{\pm} = u^{\pm}(r_0) - R_b \left.\frac{du^{\pm}}{dr}\right|_{r=r_0},$$
$$F = -\gamma L \gamma \tag{6}$$

and L is an operator function of $E - H_M$ with the eigenvalues

$$L_\nu = \frac{1}{\tilde{u}^+_\nu} \left.\frac{du^+_\nu}{dr}\right|_{r=r_0}.$$

Eq. (5) corresponds to the Nesbet's energy-modified adiabatic approximatiion [49] whereby the energy E_e in $S(E_e, R)$ is replaced by the operator $E - H_M$. He then used matrix elements of S for calculation of vibrational excitation. We will go one step further by expressing the Hamiltonian for the nuclear motion in terms of the operators entering Eq. (6).

Compare Eq. (5) with the standard expression for the S matrix in approximation of an isolated resonance

$$S = S_b - 2\pi i \frac{V \times V}{E - E_R + i\Gamma/2}$$

where S_b is the background term, V is a column of partial capture amplitudess, $\times$ sign denotes the direct product, E_R is the resonance energy, and Γ is the resonance width.

It is clear now that the partial capture amplitude can be obtained as

$$V = \frac{\gamma}{\pi^{1/2}\tilde{u}^+} \tag{7}$$

and the resonance energy and width can be expressed through the real and imaginary parts of the operator $H_I + F$. This operator can be considered as a modified Hamiltonian for

the nuclear motion which takes into account the autodetachment width. The corresponding wavefunction can be obtained by solving the Schrödinger-type equation

$$(H_I + F)\Phi^{(+)}_{\mu\mathbf{K}}(Q_r, Q) = E\Phi^{(+)}_{\mu\mathbf{K}}(Q_r, Q) \tag{8}$$

with plane plus outgoing-wave boundary condition in coordinate Q_r, where the symbol Q represents the set of variables $\{Q_1, ..., Q_{N-1}\}$, $\mathbf{K}$ the final-state wave-vector, and μ the set of vibrational quantum numbers of the fragments in the final state. For example, in the case of DEA to CF_3Cl this will be the vibrational number of the umbrella state in the CF_3 radical. Eq. (6) is equivalent to the basic equation of the nonlocal complex potential theory. Function $\Phi_{\mu\mathbf{K}}(Q_r, Q)$ is normalized to the δ-function of energy with $E = K^2/2M$ where M is the reduced mass of the products, and K is their relative momentum. Then the DEA cross section can be written as [20]

$$\sigma_{\mu\nu} = \frac{4\pi^3}{k_\nu^2}\left|\int dQ_r dQ \Phi^{(+)}_{\mu-\mathbf{K}}(Q_r, Q)V(q)\zeta_\nu(q)\right|^2 \tag{9}$$

where $|\nu\rangle = \zeta_\nu(q)$ is the initial state of the neutral molecule, k_ν is the electron momentum in the initial channel. Note that $\Phi^{(+)}_{\mu-\mathbf{K}} = \Phi^{(-)*}_{\mu\mathbf{K}}$ even for scattering by a complex potential [50], although the function $\Phi^{(-)}_{\mu\mathbf{K}}$ is no longer a solution of the Schrödinger equation with the original potential. If we are not interested in the angular distribution of the DEA products, there is no need to specify the direction of $\mathbf{K}$, and $\Phi^{(+)}_{\mu-\mathbf{K}}$ can be simply written as $\Phi^{(+)}_{\mu K}$. From now on we will be also omitting the superscript (+).

To solve Eq. (8) we rewrite it in the integral form

$$\Phi_{\mu K}(Q_r, Q) = \chi_{\mu K}(Q_r, Q) - \int G^{(+)}_E(Q_r, Q, Q'_r, Q')(\gamma L\gamma)(Q'_r, Q')\Phi_{\mu K}(Q'_r, Q')dQ'_r dQ' \tag{10}$$

where $\chi_{\mu K}(Q_r, Q)$ is the solution of the Schrödinger equation with the local potential $U^-(Q_r, Q)$, and $G^{(+)}_E(Q_r, Q, Q'_r, Q')$ is the Green's function for the same equation with the outgoing wave boundary condition. (Note that here we use the more conventional definition of the Green's operator, $G^{(+)}_E = (E + i\eta - H)^{-1}$ which has the opposite sign to that used in Ref. [43]). Although the functions $\chi_{\mu K}(Q_r, Q)$ and $\Phi_{\mu K}(Q_r, Q)$ represent the final state, it is convenient to treat them as Dirac kets.

Multiply now Eq. (10) by the Dirac bra $\langle\nu|\gamma$, where $|\nu\rangle$ is the initial vibrational state, and introduce capture amplitudes

$$x_{\nu\mu}(E) = \langle\nu|\gamma|\chi_{\mu K}\rangle, \tag{11}$$

$$y_{\nu\mu}(E) = \langle\nu|\gamma|\Phi_{\mu K}\rangle. \tag{12}$$

Then this equation can be converted into a system of linear algebraic equations for the amplitudes $y_{\nu\mu}(E)$

$$y_{\nu\mu}(E) = x_{\nu\mu}(E) - \sum_{\nu'}\langle\nu|\gamma G^{(+)}\gamma|\nu'\rangle L_{\nu'}y_{\nu'\mu}(E). \tag{13}$$

Strictly speaking, the sum over vibrational states should also include integration over the vibrational continuum. In one-dimensional case this problem can be solved either by employing the Lanczos basis [20] or by using the quasiclassical representation of the Green's operator [51]. However, in multidimensional case this task is much more challenging. Our previous calculations showed that for heavy molecules, when the density of vibrational states is high, the influence of vibrational continuum is insignificant, therefore we neglect it in the present paper. Using Eq. (9) and the connection between R-matrix surface amplitudes γ and capture amplitudes, Eq. (7), we can calculate the DEA cross section from the vibrational state ν with the formation of the products in the state μ as

$$\sigma_{\nu\mu}(E) = \frac{4\pi^2}{k_\nu^2}\left|\frac{y_{\nu\mu}(E)}{\tilde{u}_\nu^+}\right|^2. \tag{14}$$

Generally, for calculation of amplitudes $y_{\nu\mu}(E)$ it is necessary to express coordinates q in terms of Q, but in some symmetric situations this is a simple task. For example, in DEA to CY_3X we take

$$q_1 = R, \quad q_2 = r, \quad Q_r = R + \eta r, \quad Q_1 = r, \quad \eta = \frac{3m_Y}{m_C + 3m_Y}$$

where R is the C-X distance, and r is the distance between C and the plane formed by Y atoms. Accordingly

$$q_1 = Q_r - \eta Q_1, \quad q_2 = Q_1$$

IV. CAPTURE AMPLITUDES IN TERMS OF THE GREEN'S FUNCTION

For the functions entering Eq. (10) we have

$$(E - H_I)\chi_{\mu E}(Q_r, Q) = 0 \tag{15}$$

$$(E - H_I)G_E^{(+)} = \delta(Q_r - Q_r')\delta(Q - Q').$$

Expand now $\chi_{\mu E}(Q_r, Q)$ in eigenstates of the Hamiltonian of the products

$$H_p = T_p(P; Q) + U^-(\infty, Q) \tag{16}$$

defined as

$$H_p \phi_\mu(Q) = \epsilon_\mu \phi_\mu(Q). \tag{17}$$

The expansion has the form

$$\chi_{\mu E}(Q_r, Q) = N \sum_{\mu'} \psi^{(r)}_{\mu'\mu}(Q_r)\phi_\mu(Q), \tag{18}$$

where $\psi^{(r)}_{\mu'\mu}(Q_r)$ are coefficient functions regular at the origin, and N is the normalization constant. We will assume now that the kinetic energy of the relative motion of the products is given by

$$T_r = -\frac{1}{2M}\frac{d^2}{dQ_r^2}$$

where M is the reduced mass of the products. Then $\psi^{(r)}_{\mu'\mu}(Q_r)$ satisfy the following equations

$$\frac{1}{2M}\frac{d^2}{dQ_r^2}\psi_{\mu\nu} - \sum_{\mu'}[U^-_{\mu\mu'}(Q_r) + (e_\mu - E)\delta_{\mu\mu'}]\psi_{\mu'\nu} = 0, \tag{19}$$

$$U^-_{\mu\mu'}(Q_r) = \int \phi_\mu(Q)[U^-(Q_r, Q) - U^-(\infty, Q)]\phi_{\mu'}(Q)dQ. \tag{20}$$

We require ingoing and outgoing fluxes to be unity in each final channel which leads to the following asymptotic behavior of $\psi^{(r)}_{\mu'\mu}(Q_r)$

$$\psi^{(r)}_{\mu'\mu}(Q_r) \sim \delta_{\mu'\mu}\frac{e^{-iK_\mu Q_r}}{\sqrt{v_\mu}} - \frac{e^{iK_{\mu'}Q_r}}{\sqrt{v_{\mu'}}}S_{\mu'\mu} \tag{21}$$

where $S_{\mu'\mu}$ is the scattering matrix, K_μ is the asymptotic momentum for the relative motion in channel μ, and $v_\mu = K_\mu/M$ is the relative velocity in channel μ. Since Eq. (14) assumes that $\Phi^{(+)}_{\mu K}(Q_r, Q)$ is energy-normalized, we also obtain

$$N = (2\pi)^{-1/2}.$$

To calculate the capture amplitude, Eq. (11), expand first the Green's function G_E in (real) eigenstates of H_p

$$G^{(+)}_E(Q_r, Q, Q'_r, Q') = \sum_{\mu\mu'} \phi_\mu(Q)G_{\mu\mu'}(Q_r, Q'_r)\phi_{\mu'}(Q') \tag{22}$$

where the matrix Green's function $G_{\mu\mu'}(Q_r, Q'_r)$ is the solution of the system of equations (with the outgoing-wave boundary condition)

$$\frac{1}{2M}\frac{d^2}{dQ_r^2}G_{\mu\nu} - \sum_{\mu'}[U^-_{\mu\mu'}(Q_r) + (e_\mu - E)\delta_{\mu\mu'}]G_{\mu'\nu} = \delta(Q_r - Q'_r)\delta_{\mu\nu}. \tag{23}$$

The function $G_{\mu\mu'}(Q_r, Q'_r)$ can be written in the following matrix form

$$iG(Q_r, Q'_r) = \psi^{(+)}(Q_r)\psi^{(r)T}(Q'_r)\eta(Q_r - Q'_r) + \psi^{(r)}(Q_r)\psi^{(+)T}(Q'_r)\eta(Q'_r - Q_r) \tag{24}$$

where the superscript T denotes the transposition, $\eta(x)$ is the step (Heaviside) function, and $\psi^{(r)}$, $\psi^{(+)}$ are solutions of corresponding homogeneous equations (Eq. (23) with zero right-hand side). Asymptotic behavior of $\psi^{(r)}$ is given by Eq. (21), and $\psi^{(+)}$ behaves as the outgoing wave

$$\psi^{(+)} \sim \frac{1}{\sqrt{v}}e^{iKQ_r}. \tag{25}$$

According to the standard definition of the S matrix, $\psi^{\pm}$ solutions are normalized to the unit flux in each channel. Eq. (24) was used in Ref.[14] without derivation. We give the derivation in the present paper in Appendix B.

Look now at the asymptotic behavior of the integral

$$X_\nu(Q_r, Q) = \int G_E^{(+)}(Q_r, Q, Q'_r, Q')\gamma(q')\zeta_\nu(q')dQ'_r dQ' \tag{26}$$

at $Q_r \to \infty$. Then

$$G_{\mu\mu'}(Q_r, Q'_r) \sim \frac{e^{iK_\mu Q_r}}{i\sqrt{v_\mu}}\psi^{(r)}_{\mu'\mu}(Q'_r) \tag{27}$$

and

$$G_E^{(+)}(Q_r, Q, Q'_r, Q') \sim \sum_{\mu\mu'}\frac{e^{iK_\mu Q_r}}{i\sqrt{v_\mu}}\psi^{(r)}_{\mu'\mu}(Q'_r)\phi_\mu(Q)\phi_{\mu'}(Q'). \tag{28}$$

Then in the same limit

$$X_\nu(Q_r, Q) \sim \sum_{\mu'\mu}\frac{e^{iK_\mu Q_r}}{i\sqrt{v_\mu}}\phi_\mu(Q)\int \psi^{(r)}_{\mu'\mu}(Q'_r)\phi_{\mu'}(Q')\gamma(q')\zeta_\nu(q')dQ'_r dQ'$$

or

$$X_\nu(Q_r, Q) \sim \sqrt{2\pi}\sum_{\mu}\frac{e^{iK_\mu Q_r}}{i\sqrt{v_\mu}}\phi_\mu(Q)\int \chi_{\mu E}(Q'_r, Q')\gamma(q')\zeta_\nu(q')dQ'_r dQ',$$

or, using Eq. (11),

$$X_\nu(Q_r, Q) \sim \sqrt{2\pi}\sum_{\mu}\frac{e^{iK_\mu Q_r}}{i\sqrt{v_\mu}}\phi_\mu(Q)x_{\nu\mu}.$$

Using the completeness of the set $\phi_\mu(Q)$, we conclude

$$\sqrt{2\pi/v_\mu}e^{iK_\mu Q_r}x_{\nu\mu} = i\int X_\nu(Q_r,Q)\phi_\mu(Q)dQ,$$

$$\sqrt{2\pi/v_\mu}e^{iK_\mu Q_r}x_{\nu\mu} = i\int \phi_\mu(Q)G_E^{(+)}(Q_r,Q,Q_r',Q')\gamma(q')\zeta_\nu(q')dQ_r'dQ'dQ. \tag{29}$$

Therefore calculation of the zero-order capture amplitude $x_{\nu\mu}$ is reduced to calculation of a $2N-1$-dimensional integral containing the Green's function at large Q_r and matching the result to the left-hand side of Eq. (29). Although in quantum calculations the capture amplitude can be evaluated directly from Eq. (11), representation (29) is useful for semiclassical calculations. The matrix elements of the Green's function are reduced to calculation of $2N$-dimensional integral

$$\langle\nu|\gamma G_E^{(+)}\gamma|\nu'\rangle = \int \zeta_\nu(q)\gamma(q)G_E^{(+)}(Q_r,Q,Q_r',Q')\gamma(q')\zeta_{\nu'}(q')dqdq'. \tag{30}$$

V. QUANTUM CALCULATIONS OF THE CAPTURE AMPLITUDE AND THE MATRIX ELEMENTS OF THE GREEN'S FUNCTION

Eqs. (29), (30) do not involve the explicit form of the Green's function which can be calculated by quantum-mechanical or semiclassical methods. In quantum-mechanical calculations we use the exact expresion, Eq. (22), and then

$$\langle\nu|\gamma G_E^{(+)}\gamma|\nu'\rangle = \sum_{\mu\mu'}\int \lambda_{\mu\nu}(Q_r)G_{\mu\mu'}(Q_r,Q_r')\lambda_{\mu'\nu'}(Q_r')dQ_rdQ_r' \tag{31}$$

where

$$\lambda_{\mu\nu}(Q_r) = \int \phi_\mu(Q)\gamma(Q_r,Q)\zeta_\nu(q)dQ. \tag{32}$$

We can also use Eq. (11) to find the capture amplitude as

$$x_{\nu\mu}(E) = \frac{1}{\sqrt{2\pi}}\sum_{\mu'}\int \psi_{\mu'\mu}^{(r)}(Q_r)\lambda_{\mu'\nu}(Q_r)dQ_r. \tag{33}$$

which agrees with the Green's function representation (29).

To construct the matrix Green's function, $G_{\mu\mu'}(Q_r,Q_r')$, we need to obtain matrices of regular and outgoing-wave solutions, $\psi^{(r)}$ and $\psi^{(+)}$. To find $\psi^{(r)}$ matrix, we first integrate outward the homogeneous coupled equations with regular boundary conditions at the origin

and form a corresponding square matrix $\psi^{(a)}$. At some intermediate distance ρ_0, we match this matrix with the matrix $\psi^{(r)}$ satisfying the required boundary conditions at $Q_r \to \infty$

$$\psi^{(a)}C = \psi^{(-)} - \psi^{(+)}S \quad \text{at} \quad Q_r = Q_{\rho_0}, \tag{34}$$

and a similar equation for derivatives, where C is a matrix of coefficients which should be determined, together with the S matrix, from matching conditions. Solutions $\psi^{\pm}$ are obtained by the inward integration of the coupled homogeneous equations from the asymptotic region to $Q_r = Q_{r0}$. Since exponentially growing solutions in the closed channels are unphysical, matrices $C, \psi^{(-)}$ and S in Eq. (34) are rectangular with N_μ rows and N_o columns, where N_μ is the total number of product channels, and N_o is the number of open channels. After S and C are found, $\psi^{(r)}$ is calculated as $\psi^{(a)}C$. The computational scheme is described in Appendix A for the generic case of a CY_3X molecule.

VI. SEMICLASSICAL APPROACH

Calculation of the matrix elements of the Green's function entering Eq. (13) presents a big computational challenge. Although for specific calculations in the 2d case we use the exact approach, as discussed in the next section, it is worth exploring semiclassical methods since going beyond 3d case within the formalism of quantum mechanics becomes practically infeasible. We remind the reader that the quasiclassical theory of DEA [51] is based on the WKB solution of the one-dimensional Schrödinger equation, and the semiclassical theory starts from classical trajectories which serve as an input for calculation of the van Vleck-Gutzwiller propagator [52, 53] (VVG). In contrast to the former, the latter version can be easily generalized to multidimensional case. In our notations a classical trajectory can be written as

$$\mathbf{Q} = \mathbf{Q}(\mathbf{Q}', \mathbf{P}', t)$$

where $\mathbf{Q} = \{Q_r, Q\}$ represents the totality of all internuclear coordinates, and $\mathbf{P} = \{P_r, P\}$ conjugated momenta, and $\mathbf{Q}', \mathbf{P}'$ are initial coordinates and momenta. Introducing the principal Hamiltonian function describing the propagation from the initial point in the coordinate space $\mathbf{Q}'$ to the final point $\mathbf{Q}$

$$R(\mathbf{Q}', \mathbf{Q}, t) = \int_0^t L(t')dt'$$

where L is the Lagrangian, we can write the VVG propagator as

$$G_{VVG}(\mathbf{Q}',\mathbf{Q},t) = -\frac{i}{(2\pi i)^{N/2}}\exp\{i[R(\mathbf{Q}',\mathbf{Q},t) - \lambda\pi/2]\}\left|\det\frac{\partial\mathbf{Q}}{\partial\mathbf{P}'}\right|^{-1/2} \quad , \quad t>0 \tag{35}$$

where λ is the Maslov index [54] indicating how many times the determinant under the square root turns to 0. The stationary Green's function with outgoing-wave boundary condition is given by the Fourier transform

$$G_E^{(+)}(\mathbf{Q}',\mathbf{Q}) = \int_0^\infty G_{VVG}(\mathbf{Q}',\mathbf{Q},t)e^{iEt}dt \tag{36}$$

and therefore, the matrix elements of $\gamma G\gamma$ are given by

$$\begin{aligned}\langle\nu'|\gamma G\gamma|\nu\rangle = -\frac{i}{(2\pi i)^{N/2}}\int d\mathbf{Q}d\mathbf{Q}'\zeta_{\nu'}(\mathbf{q})\gamma(\mathbf{q}')\zeta_\nu(\mathbf{q})\gamma(\mathbf{q}) \\ \int_0^\infty dt\exp\{i[R(\mathbf{Q}',\mathbf{Q},t) + Et - \lambda\pi/2]\}\left|\det\frac{\partial\mathbf{Q}}{\partial\mathbf{P}'}\right|^{-1/2}\end{aligned} \tag{37}$$

A. SEMICLASSICAL INITIAL VALUE REPRESENTATION

The major difficulty in calculating integral (37) is the so-called root-search problem [55, 56]. For each set of $\mathbf{Q}'$ and $\mathbf{Q}$ we have to find the initial momenta $\mathbf{P}'$ which can be a tedious task in the multidimensional case. To solve this problem Miller proposed to use the Initial Value Representation (IVR)[57] by switching to the integration variables $\mathbf{Q}',\mathbf{P}'$. The integration is reduced then to

$$\begin{aligned}\langle\nu'|\gamma G\gamma|\nu\rangle = -\frac{i}{(2\pi i)^{N/2}}\int d\mathbf{Q}'\zeta_{\nu'}(\mathbf{Q}')\gamma(\mathbf{Q}')\int d\mathbf{P}' \\ \int_0^\infty dt\zeta_\nu(\mathbf{Q}(\mathbf{Q}',\mathbf{P}',t))\gamma(\mathbf{Q}(\mathbf{Q}',\mathbf{P}',t))\exp\{i[R(\mathbf{Q}',\mathbf{P}',t) + Et - \lambda\pi/2]\}\left|\det\frac{\partial\mathbf{Q}}{\partial\mathbf{P}'}\right|^{1/2}\end{aligned} \tag{38}$$

Now for each set of $\mathbf{Q}',\mathbf{P}'$ we run just one trajectory allowing us to calculate the time integral. The number of required trajectories is determined by the number of points in the initial phase space $(\mathbf{Q}',\mathbf{P}')$. An additional advantage of representation (38) is that the integrand does not contain singularities associated with the zeros of the Jacobian $\partial\mathbf{Q}/\partial\mathbf{P}'$. A useful representation for the zero-order capture amplitude $x_{\nu\mu}(E)$ can be obtained from the spectral representation of the diagonal matrix elements of the Green's function

$$\langle\nu'|\gamma G\gamma|\nu\rangle = -\sum_\mu\int d\mathbf{K}\frac{\langle\nu|\gamma|\mathbf{K}\mu\rangle\langle\mu\mathbf{K}|\gamma|\nu\rangle}{K^2/2M + e_\mu - E - i\eta} \tag{39}$$

where $\mathbf{K}$ is the momentum for the relative motion of the products, e_μ are the energy eigenvalues of the products and $|\mathbf{K}\mu\rangle$ are eigenstates of the final-state Hamiltonian H_f. Assuming again that the products dissociate along the straight line, we can replace these eigenstates by $\chi_{\mu E}(\mathbf{Q})$ normalized to the δ-function of energy. Taking then the imaginary part of the both sides of Eq. (39), we obtain

$$Im\,\langle\nu|\gamma G\gamma|\nu\rangle = -\pi\sum_\mu |\langle\nu|\gamma|\chi_{\mu E}\rangle|^2 \tag{40}$$

This equation allows us to check the quality of the semiclassical calculations of the Green's function by verifying that the left-hand-side is negative and agrees with the right-hand-side calculated by the quantum mechanical methods.

B. Stationary semiclassical method

In the stationary formalism the IVR method exhibits an apparent deficiency: the necessity of numerical time integration of a rapidly oscillating function. This integration cannot be peformed by the stationary phase method since the initial wavefunction in Eq. (38) implicitly depends on t. To take advantage of the stationary phase method, we return to the van Vleck-Gutzwiller propagator, Eq. (35). Calculating the time integral by the stationary phase method, we obtain the known result for the 1D semiclassical energy-dependent Green's function

$$G(R,R') = \frac{-iM}{\sqrt{|P(R)P(R')|}}\sum e^{i[S(R,R')-\sigma\pi/2]} \tag{41}$$

where $R = Q_r$ is the reaction coordinate in the 1d case. Here $P(R)$ and $P(R')$ are the momenta at R, R'. $S(R,R')$ is the reduced or abbreviated action ($S = R + Et$). The summation is done over all classical paths connecting R' and R. σ in the exponent counts the number of turning points encountered by a trajectory. By substituting Eq. (41) in Eq. (29), we have

$$x_\nu^{SC} = \sqrt{M}e^{-iKR}\int dR'\frac{1}{\sqrt{|P(R')|}}\gamma(R')\zeta_\nu(R')\sum e^{i[S(R,R')-\sigma\pi/2]}. \tag{42}$$

Note that here $K = |P(R)|$. The root search for trajectories between R' and R can be avoided by running multiple trajectories from each R' and ending at some asymptotic R (similar approach will be taken in the multidimensional case). These trajectories must

satisfy the relation: $E = P'^2/2m + U_{1D}^-(R')$ at each initial R', where E is the total energy. The integration in Eq. (42) can be regularized at the turning points by switching to the momentum variable

$$dR' = \left| P' \left(\frac{\partial U_{1D}^-}{\partial R'} \right)^{-1} \right| dP'/M,$$

assuming a repulsive potential in the region of integration. For matrix elements of the Green's function, we directly evaluate the SC-IVR expression given by Eq. (38) in sec. VI A. As pointed out in sec. VI A, another approach to computing the capture amplitudes and the matrix elements is the quasiclassical (WKB) approximation [51, 60–62]. In this method, in addition to writing down the wavefunctions in terms of the WKB solutions, the spatial integrals are evaluated by using the stationary points determined by the Franck-Condon principle [62, 63].

The generalization to the multidimensional case is straightforward: To compute the semiclassical capture amplitudes, we use the stationary Green's function which is obtained by applying the stationary phase approximation (SPA) on the time integral of Eq. (36). Then the multidimensional stationary Green's function reads

$$\begin{aligned} G_E(\mathbf{Q}', \mathbf{Q}) = -\frac{i}{(2\pi i)^{\frac{N-1}{2}}} \sum_{t^*} \left| \det \frac{\partial \mathbf{Q}}{\partial \mathbf{P}'} \right|^{-1/2} \left| -\frac{\partial E}{\partial t^*} \right|^{-1/2} \\ \times \exp\{i[R(\mathbf{Q}', \mathbf{Q}, t^*) + Et^* - \lambda\pi/2 - \sigma\pi/2]\}, \end{aligned} \tag{43}$$

where the summation is over all t^* which are the solutions of the stationary phase condition,

$$\frac{\partial R(\mathbf{Q}', \mathbf{Q}, t)}{\partial t} + E = 0. \tag{44}$$

The constant σ in the exponent of Eq. (43) is 0 or 1 if $-\partial E/\partial t^*$ is positive or negative, respectively. According to the Hamilton-Jacobi theory, the solutions, t^*, to the stationary phase condition in Eq. (44) are the classical trajectories with energy E and connecting the points $\mathbf{Q}'$ and $\mathbf{Q}$ with travel time t^*. Then the capture amplitude for a given E can be computed using Eq. (29) by doing Monte-Carlo integration where an ensemble of trajectories with energy E is propagated up to an asymptotic distance Q_r. For a given outgoing channel μ, the ensemble of trajectories must also produce final CY_3 fragments with energy close to the corresponding quantum value : $(\mu+1/2)\omega_{2f}$. Figure 6 shows the comparison between the 2D quantum and semiclassical capture amplitudes for capturing an electron in the ground state of the neutral molecule and producing CY_3 fragments in the ground state. About 5×10^4

trajectories were used in the semiclassical calculations. Trajectories which have caustic divergence on the final point of integration, i.e., at (Q_r, Q) are omitted from the Monte-Carlo sum.

VII. MODEL POTENTIAL ENERGY SURFACES AND R-MATRIX SURFACE AMPLITUDE

For a molecule of the type CY_3X, we use the following 2D model potentials which are functions of the inter-nuclear separation of C−X (= R) and C−Y_3 (= r) [26], as shown in Fig. 1 (note that the C−Y length is kept constant in the present calculations)

$$U^0(R,r) = U^0_{1D}(R) + \frac{1}{2}\left[k^0 + (k^0_e - k^0)e^{-\Gamma^0(R-R_e)}\right]\left[r - r^0_{ef} - (r^0_e - r^0_{ef})e^{-\Delta^0(R-R_e)}\right]^2, \quad (45)$$

$$U^-(R,r) = U^-_{1D}(R) + \frac{1}{2}\left[k + (k_e - k)e^{-\Gamma(R-R_e)}\right]\left[r - r_{ef} - (r_e - r_{ef})e^{-\Delta(R-R_e)}\right]^2, \quad (46)$$

where $U^0(R,r)$ and $U^-(R,r)$ are neutral and anion potential surfaces. At the equilibrium value of R, $R = R_e$, apart from some constants, the neutral and anion potential give the harmonic terms $k^0_e(r-r^0_e)^2/2$ and $k_e(r-r_e)^2/2$ respectively. The constants in the exponents; $\Gamma^0, \Gamma, \Delta^0$ and Δ are positive. Therefore, as $R \to \infty$, the neutral and anion potentials reduce to their harmonic oscillator limits; $k^0(r - r^0_{ef})^2/2$ and $k(r - r_{ef})^2/2$, respectively. k^0, k, r^0_{ef} and r_{ef} are the force constants and equilibrium C-Y_3 separations at $R \to \infty$. The potential curves depending on only R are given in terms of the 1D Morse potentials,

$$V^0_{1D}(R) = A(e^{-\alpha(R-R_e)} - 1)^2 \quad (47)$$

$$U^-_{1D}(R) = Be^{-2\beta(R-R_e)} - Ce^{-\beta(R-R_e)} + D. \quad (48)$$

We use the following parameterization for the R-matrix surface amplitude [23] for both 1D and 2D calculations.

$$\gamma_{1D}(R) = a_0 + \frac{a_1}{e^{-\zeta(R-R_e)} + a_2}, \quad (49)$$

For the values of the parameters; $A, B, C, D, \alpha, \beta, a_0, a_1, a_2$ and ζ in Eqs. (47)-(49), we use the data given in [23](model 2). In order to obtain most accurate results with many vibrational modes, the surface amplitude function must include the dependence on all internal coordinates. As was stressed in Introduction, it is not the goal of the present paper to

calculate all fixed-nuclei parameters *ab initio*. Instead we will investigate the effect of r dependence of γ by representing it in the following parametric form

$$\gamma_{\pm}(R,r) = \gamma_{1D}(R)[1 \pm a(r - r_e)] \tag{50}$$

and studying the dependence of the DEA cross sections on parameter a.

Figure 2 shows the 1D neutral and anion curves as function of R, and 1D cuts of the 2D potential surfaces which are given by Eqs. (45) and (46).

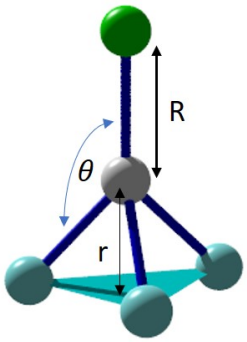

FIG. 1: Internal coordinates of the CY_3X molecule. R, the reaction coordinates, is the distance between the C and X atoms. r is the perpendicular distance between the C atom and the plane formed by 3 Y atoms.

The total kinetic energy of the nuclear motion in terms of the internal coordinates R and r has the form [26]

$$T(R,r) = \frac{1}{2}\mu_1 \dot{R}^2 + \frac{1}{2}\mu_2 \dot{r}^2 + \mu_3 \dot{R}\dot{r} \tag{51}$$

where,

$$\mu_1 = \frac{m_{\rm X}(m_{\rm C} + 3m_{\rm Y})}{m_t} \quad ; m_t = m_{\rm C} + m_{\rm X} + 3m_{\rm Y}$$

$$\mu_2 = 3m_{\rm Y}(\cot^2\theta + \frac{m_{\rm C} + m_{\rm X}}{m_t})$$

$$\mu_3 = \frac{3m_{\rm Y}m_{\rm X}}{m_t}$$

θ is the equilibrium angle of the X−C−Y bend. $m_{\rm C}, m_{\rm X}$ and $m_{\rm Y}$ are the masses of the C,X and Y atoms, and m_t is the total mass. Terms in the kinetic energy can be decoupled by introducing the reaction coordinate given by [26],

$$\rho = R + \eta r, \quad \eta = \frac{3m_{\rm Y}}{m_{\rm C} + 3m_{\rm Y}}. \tag{52}$$

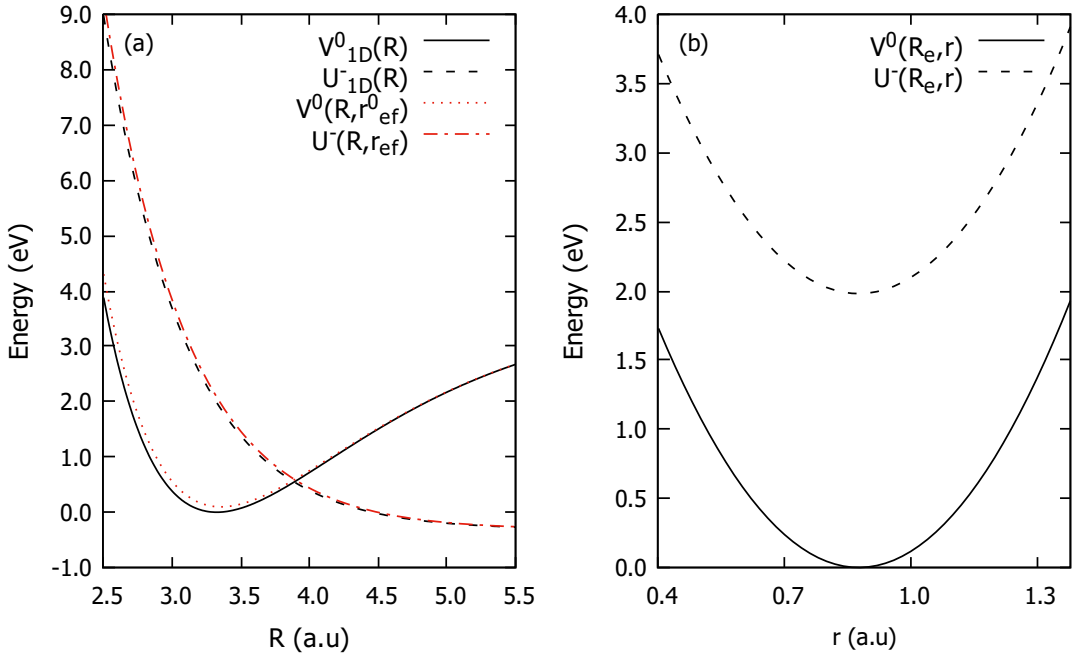

FIG. 2: Panel (a). Plots of 1D neutral and anion potential curves V^0_{1D} and U^-_{1D}, respectively, are compared against the corresponding 1D cuts of the 2D potential surfaces, $V^0(R,r)$ and $U^-(R,r)$ along a fixed C−Y_3 separation. Panel (b). 1D cuts of the neutral and anion surfaces along the equilibrium C−X separation: R_e.

Therefore the kinetic energy term now reduces to

$$T(\rho,r) = \frac{1}{2}\mu_\rho \dot{\rho}^2 + \frac{1}{2}\mu_r \dot{r}^2 \tag{53}$$

where μ_ρ is the mass corresponding to the motion of ρ coordinate and μ_r is the mass corresponding to the umbrella motion of the CY_3 radical.

$$\mu_\rho = \frac{m_X(m_C + 3m_Y)}{m_t}$$

$$\mu_r = 3m_Y(\cot^2\theta + \frac{m_C}{m_C + 3m_Y})$$

The two normal modes of vibrations in the ground state and weakly excited states of the neutral molecule can be obtained by a harmonic approximation to the potential in Eq. (45). The exact eigenstates and eigenenergies of the target molecule can be found by calculating the matrix elements of the Hamiltonian $H_M = T + U^0(\rho,r)$ in a suitable basis. In the present calculations the basis is chosen as products of the eigenfunctions of the 1D harmonic Hamiltonians corresponding to the independent motion along ρ and r coordinates. Table I gives the vibrational frequencies ω_2 (CY_3 s-deform or "umbrella") and ω_3 (C−X s-stretch) for lower states which were fitted to measued normal mode frequencies; ω_{2f} is the vibrational

frequency of the free CY_3 radical. For higher states normal modes mix and cannot be identified as pure s-deform and C−X s-stretch.

TABLE I: Normal mode frequencies calculated using the model potential energy surface. For comparison, the values for CF_3Cl molecules are also presented.

Vibrational mode(cm^{-1})	Present work	CF_3Cl
ω_2	775.5	775.12 [58]
ω_3	468.9	463.33 [58]
ω_{2f}	701.0	701 [59]

VIII. 1D APPROXIMATION RESULTS

Figure 3 compares the quantum and semiclassical capture amplitudes which are computed using Eq. (33) and Eq. (42), respectively. Comparison of the quantum and semiclassical matrix elements of the Green's function is shown in Fig. 4. In both Figs. 3 and 4, we show the corresponding quasiclassical results which are obtained by using the expressions derived in ref. [62]. DEA cross sections obtained from the 1D capture amplitudes and matrix elements are shown in Fig. 5. The excellent agreement between the one-mode quantum and semiclassical results gives us a confidence in reliability of semiclassical approach in multimode DEA calculations. The peak values of present quantum and semiclassical cross sections are higher than the previously published quasiclassical results [23]. This difference can be attributed to the difference in the matrix elements shown in Fig. 4. With regard to comparison with experiment [38, 41], our results are not qualitatively different from the previous calculations: they show good agreement with experiment at $T = 300$ K, but the low-energy peak at $T = 800$ K is too narrow as compared with experiment.

IX. 2D APPROXIMATION RESULTS

In two mode calculation of the exact matrix elements, both regular and irregular solution matrices: ($\psi^{(r)}$ and $\psi^{(+)}$) of the homogeneous coupled channel equation are required in the full integration range of ρ. Method of computing the regular solution is given in sec. V

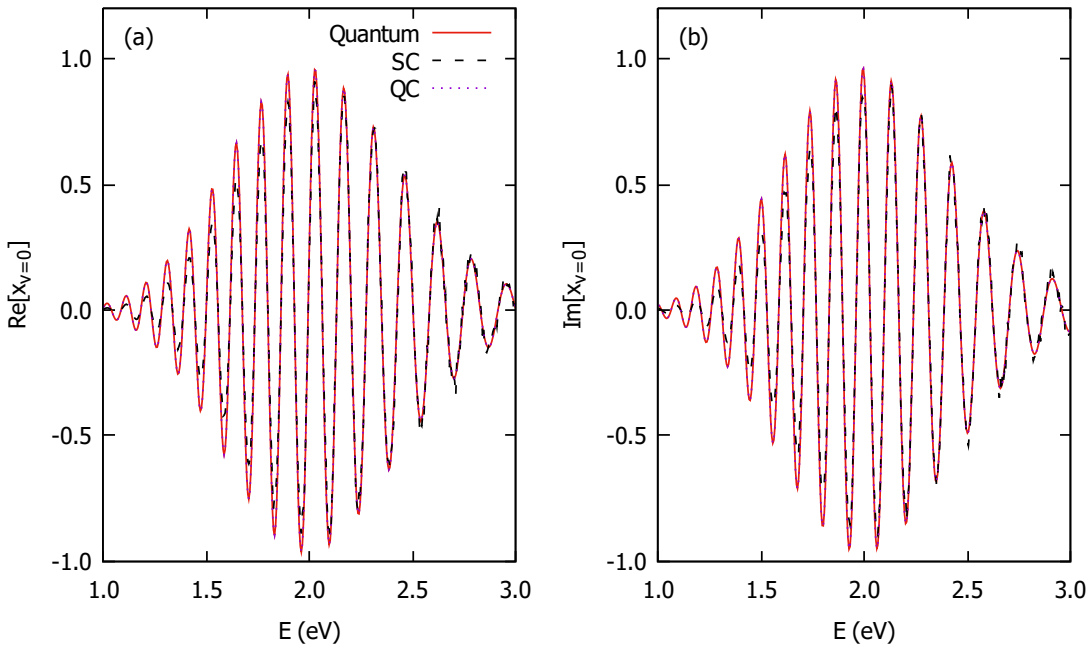

FIG. 3: (Color online) Panels (a) and (b) compare the real and imaginary parts of quantum, semiclassical (SC) and quasiclassical (QC) capture amplitudes to the ground state, as a function of the incident energy.

and is similar to the description given in ref. [14]. In the present calculation, the irregular solution must also be integrated inward from the asymptotic region deep into the classically forbidden region. Since the solutions of the coupled equation (Eq. (19) in sec. IV) grow exponentially in the closed channels, the solutions become numerically unstable as the number of closed channels increases. Therefore, it is necessary to maintain the stability and linear independence of the solutions with respect to the increasing number of open and closed channels. In the present non-local calculations we use about five open channels including only one closed channel and do integration with a small step size ($h \approx 10^{-4} - 10^{-3}$) to avoid such numerical issues. In the two-mode version of the local theory, Tarana *et al* [15] employed the exterior complex scaling (ECS) method with a discrete variable representation (DVR) basis [64] to generate stable solutions of the multi-channel problem. Fortunately, in the semiclassical approach such numerical issues are not encountered. Figure 7 compares the quantum and semiclassical matrix elements of the Green's function. The convergence of the quantum calculations is reached when the final number of umbrella channels ($\mu_{max} + 1$) is about 4 or 5 where μ_{max} is the maximum vibrational quantum number for umbrella motion. It is important to note that the semiclassical calculation of the matrix elements has no limitation in the number of open and closed channels.

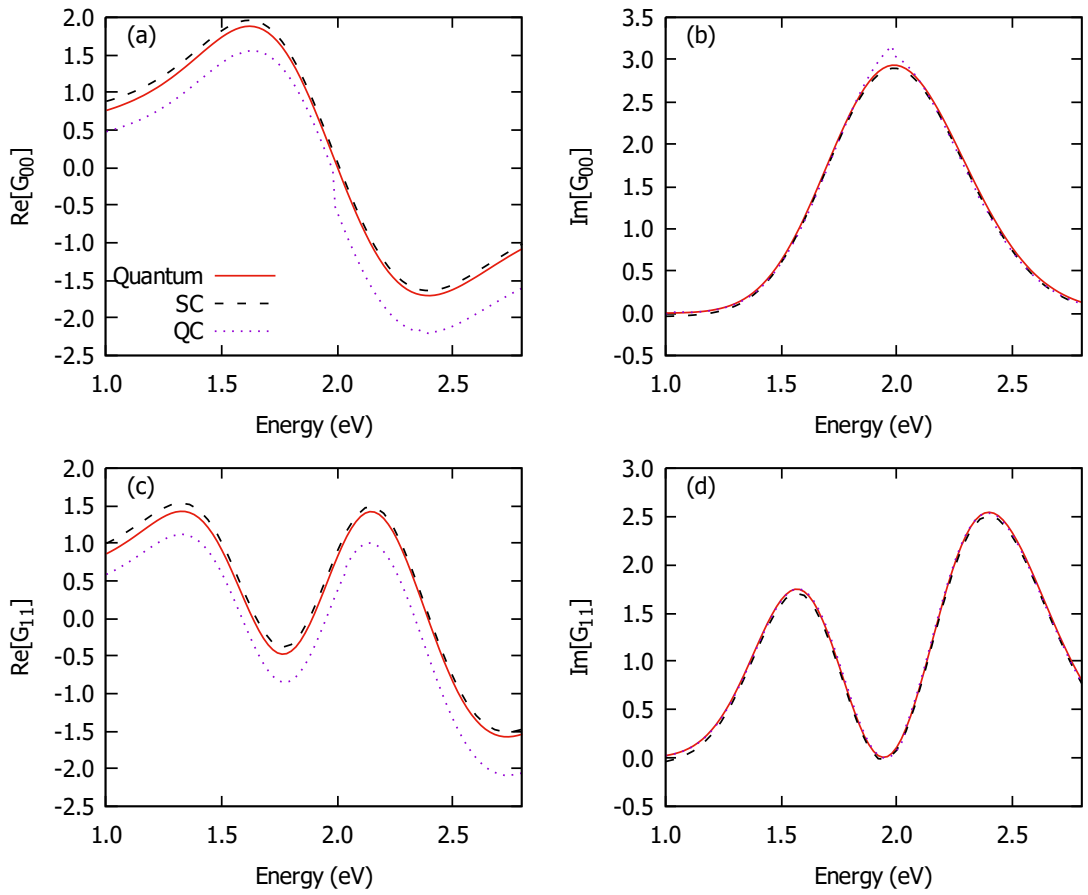

FIG. 4: (Color online) Panels (a) -(d) compare the real and imaginary parts of the quantum, semiclassical (SC) and quasiclassical (QC) matrix elements of the Green's function as function of the incident electron energy.

The quantum and semiclassical temperature-averaged cross sections are obtained by using a 200×200 matrix Green's function. In semiclassical approach, calculation of such a large complex matrix with oscillatory functions is computationally challenging (the well-known "sign problem"). For example, Monte-Carlo evaluation of the matrix elements requires a large number of classical trajectories to reach the convergence. Since we need matrix elements between different vibrational levels, special techniques like the time-averaging of the SC-IVR integral [65] or Filinov transformation [66], cannot be used to reduce the number of trajectories in the present problem. However, there are two simplifying factors: First the multi-dimensional SC-IVR integral can be calculated only once for all energies. Second, the columns of the Green's function matrix can be conveniently computed in a parallel computer environment. With these realizations, we calculate the SC-IVR integral directly on a grid using about 5×10^5 trajectories.

In Fig. 8 we show the temperature-averaged DEA cross sections for the 2D model at two

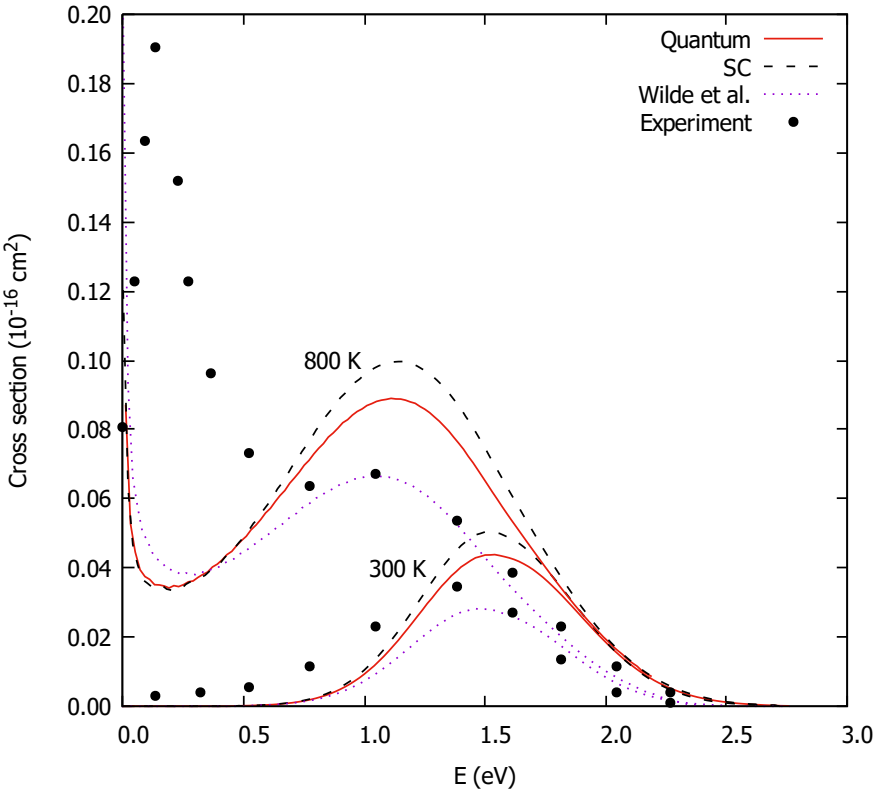

FIG. 5: (Color online) Temperature averaged DEA cross section versus the incident electron energy. Quantum and semiclassical cross sections are compared with the experiment [38, 41] and previous 1D quasiclassical calculations [23].

different temperatures (300 K and 800 K). In 2D calculations, the cross sections are summed over the final umbrella channels. The 2D cross sections are significantly higher than the 1D results as previously reported in the local approximation [14]. With more accurate potential energy surfaces (PES) for CF_3Cl, Tarana *et al.* [15] obtained close agreement between the 1D and 2D cross section in the local approximation. However, in the present work, we do not use the exact PES for the anion and the neutral molecule as our major concern is to develop the multimode nonlocal theory. for computing DEA cross section. The overall agreement of the semiclassical two-mode cross section with the quantum results suggests the validity of the semiclassical approach in DEA calculations.

So far in our 2D calculations we have used the parameterized R-matrix surface amplitude which depends only on the C−Cl separation. Figure 9 investigates how the 2D cross section (at 800 K) varies if the R-matrix surface amplitude depends on both internal coordinates as shown in Eq. (50). No much change in the low-energy peak is observed.

Figure 10 shows the DEA cross section to each final umbrella channel. In the given

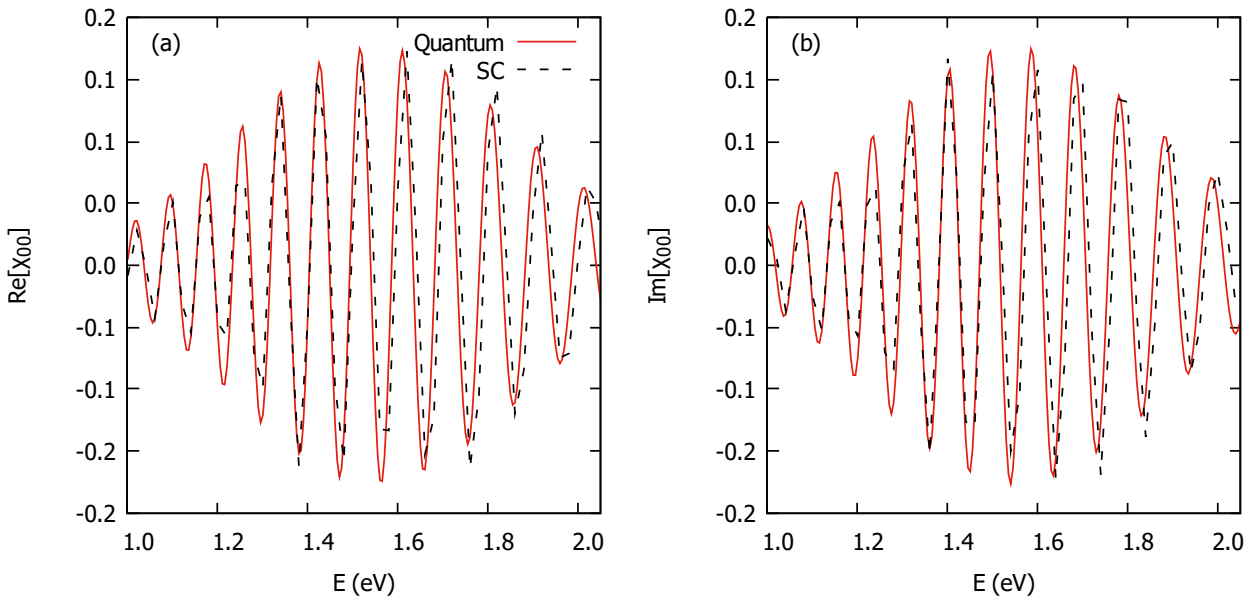

FIG. 6: (Color online)As a function of the incident electron energy, panels (a) and (b) compare the real and imaginary parts of 2D quantum and semiclassical (SC) capture amplitudes to the ground state of the neutral molecule and producing CY_3 fragments in the ground state.

incident electron energy range, results show that the most of the free CY_3 radicals produced are in the vibrationally excited states with the highest population at $\mu = 3$. In Fig. 11 we show how the DEA cross section varies as function of energy when the target molecule is in the first lowest excited states. These excited states are mixtures of C−Cl stretch and CF_3 umbrella vibrational quantum numbers. The resonance peak shifts towards the low-electron energies when the target molecule is in an excited state. We can also see a significant enhancement in the cross section compared to when the target molecule is in an ground state. We can also fix the incident electron energy and analyze how the DEA cross section varies as a function of the vibrational energy of the target molecule. We show the corresponding results in Fig. 12 for two electron energies. For low vibrational temperatures (< 1000 K), the two-mode DEA cross section is seen to be higher than the one-mode cross section. As the vibrational temperature increases, two-mode cross section more or less follow the trend in one-mode results.

X. CONCLUSIONS

In the present paper, we developed the multimode nonlocal theory to treat DEA to polyatomic molecules when there are more than one degree of vibrational freedom. We also

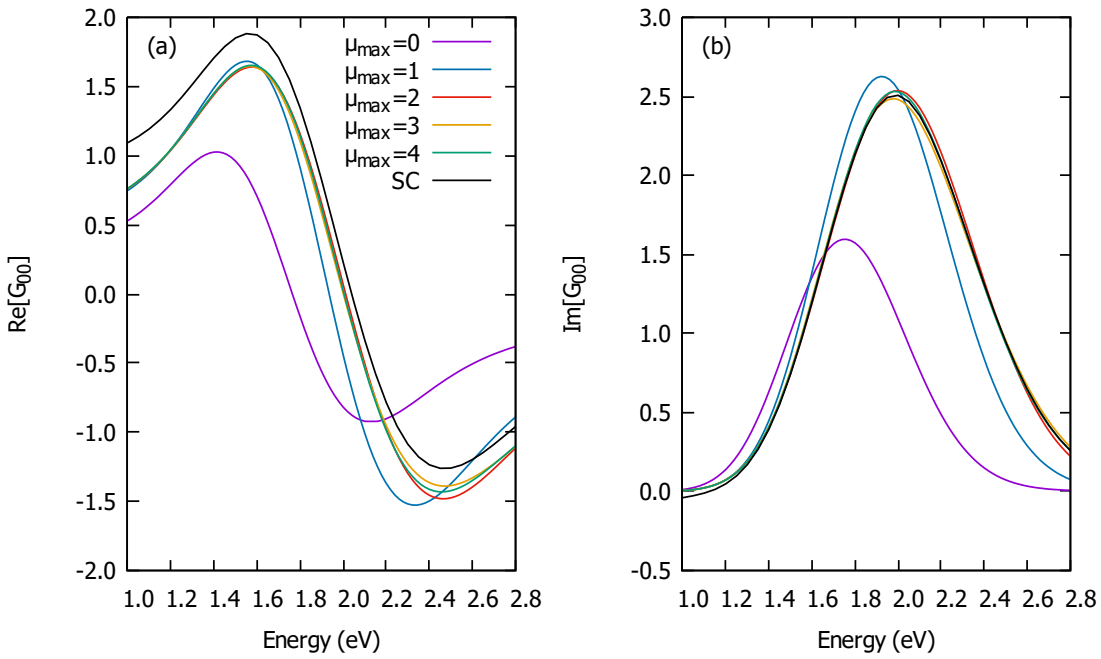

FIG. 7: (Color online)Panels (a) and (b) compare the real and imaginary parts of the ground-state matrix element as a function of electron energy. Convergence of the quantum matrix elements is achieved by increasing the number of final umbrella channels. Semiclassical result is also shown.

introduced a semiclassical version of the nonlocal theory. By using model potential energy surfaces, we obtained both quantum and semiclassical DEA cross sections for the molecule CF_3Cl.

The nonlocal theory developed in the present work can be applied to molecules having more than two vibrational modes. However, as justified in our results, the semiclassical approach to compute multimode DEA cross section is more favored compared with the full quantum treatment. As the number of dimensions grows, it is easier to run classical trajectories compared to solving the coupled Schrodinger equation. In the current two-mode semiclassical approach, we evaluated the capture amplitude using the Monte-Carlo integration, and the SC-IVR matrix elements using grid integration in 4-d phase-space (in addition to the time integration). Suitable and efficient Monte-Carlo schemes must be explored in order to compute the capture amplitudes and matrix elements in higher dimensions than required in the present calculations.

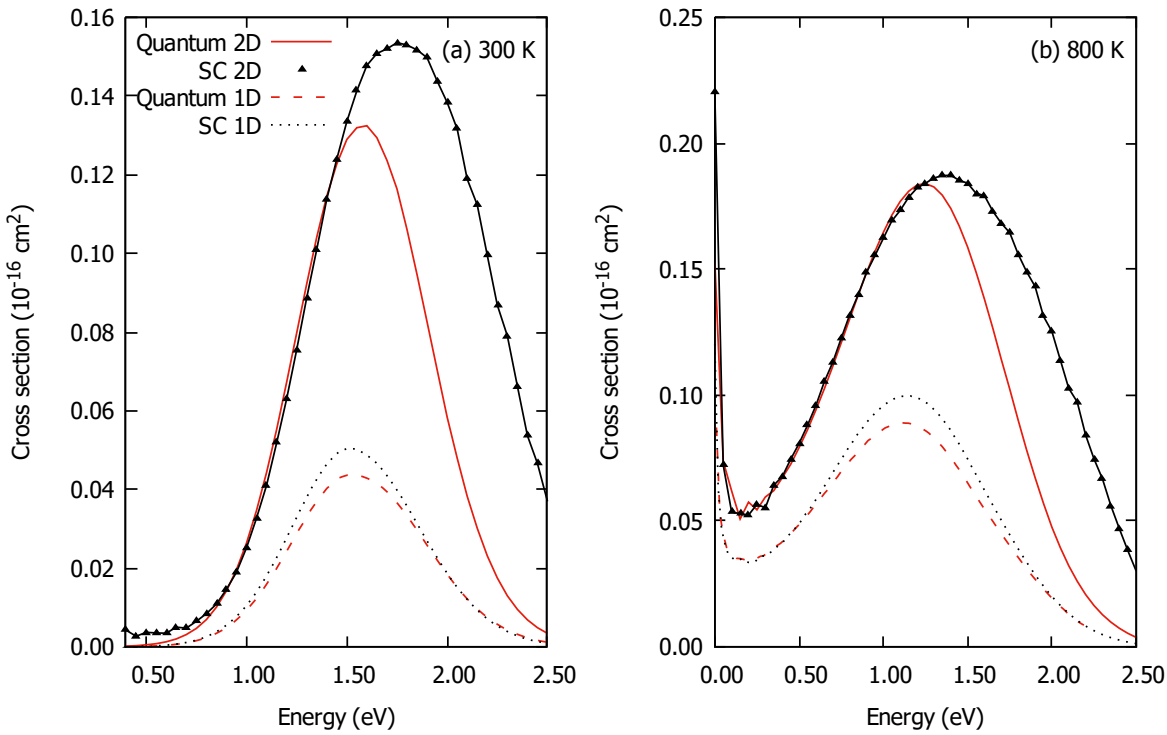

FIG. 8: Panel (a). Temperature-averaged DEA cross section at 300 K. Both quantum and semiclassical 2D cross sections are shown and compared with the results from the 1D approximation. Panel (b). Same as in Panel (a), but with the temperature at 800 K.

XI. ACKNOWLEDGMENTS

This work was supported by the US National Science Foundation under Grant No. PHY-1803744. The two-mode SC-IVR calculations were done utilizing the Holland Computing Center of the University of Nebraska, which receives support from the Nebraska Research Initiative.

APPENDIX A: COMPUTATIONAL SCHEME

We need to calculate the zero-order capture amplitude, Eq. (33), and matrix elements of the Green's function, Eq. (31). For notational convenience we introduce

$$\bar{x}_{\nu\mu} = (2\pi)^{1/2} x_{\nu\mu}.$$

We introduce now matrices with respect to asymptotic channels μ and the following notations: $\bar{x}^{\nu}$ and λ^{ν} are columns with elements $\bar{x}_{\nu\mu}$ and $\lambda_{\mu\nu}$, and ψ is a square matrix with the

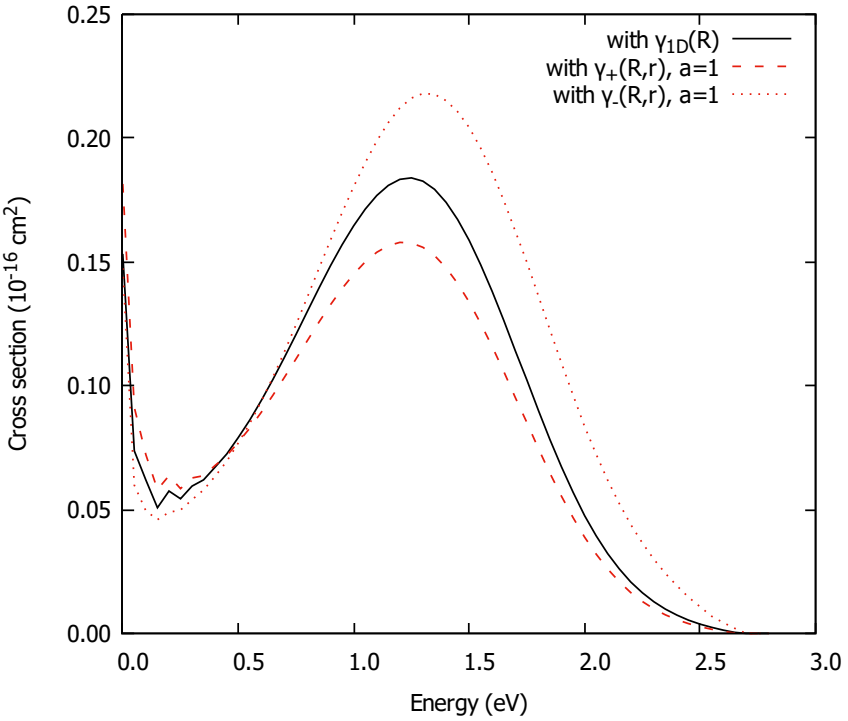

FIG. 9: Comparison of the temperature-averaged cross sections (at 800 K) which are computed using 1D and 2D approximations for the R-matrix surface amplitude function.

elements $\psi_{\mu'\mu}$. Then

$$\bar{x}^\nu = \int_0^\infty \psi^{(r)T}(\rho)\lambda^\nu(\rho)d\rho$$

where the superscript T means transposition. For $\psi^{(r)}$, according to Eq. (34), we use

$$\begin{aligned} \psi^{(r)}(\rho) &= \psi^{(a)}(\rho)C \quad \text{for} \quad \rho < \rho_0 \\ \psi^{(r)}(\rho) &= \psi^{(-)}(\rho) - \psi^{(+)}(\rho)S \quad \text{for} \quad \rho > \rho_0. \end{aligned} \tag{A1}$$

Then

$$\bar{x}^\nu = C^T J^\nu(\rho_0) + I^{(-)\nu}(\rho_0) - SI^{(+)\nu}(\rho_0) \tag{A2}$$

where

$$J^\nu(\rho) = \int_0^\rho \psi^{(a)T}(\rho')\lambda^\nu(\rho')d\rho'$$

$$I^{(\pm)\nu}(\rho) = \int_\rho^\infty \psi^{(\pm)T}(\rho')\lambda^\nu(\rho')d\rho'$$

and the symmetry of the S matrix has been used.

We will turn now to calculation of the Green-function matrix. According to Eqs. (24),

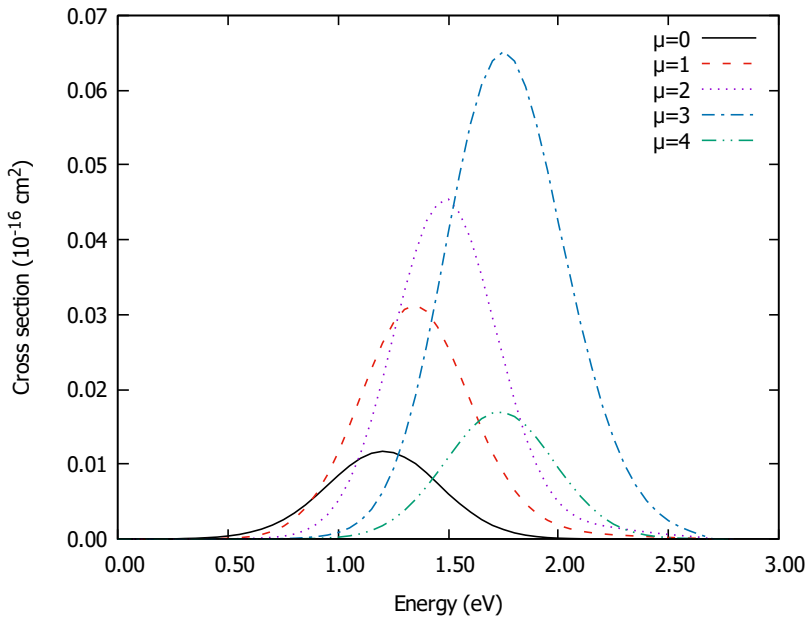

FIG. 10: (Color online) DEA cross sections (Quantum) to different final umbrella channels corresponding the CY_3 vibrations.

(31)

$$i\langle\nu'|\gamma G_E^+\gamma|\nu\rangle = \int_0^\infty d\rho\lambda^{\nu T}(\rho)[\psi^{(+)}(\rho)\int_0^\rho \psi^{(r)T}(\rho')\lambda^{\nu'}(\rho')d\rho' + \psi^{(r)}(\rho)\int_\rho^\infty \psi^{(+)T}(\rho')\lambda^{\nu'}(\rho')d\rho'. \tag{A3}$$

Using again expressions (A1) for $\psi^{(r)}$, we obtain

$$\begin{aligned} i\langle\nu'|\gamma G_E^+\gamma|\nu\rangle = \int_0^\infty d\rho\lambda^{\nu T}(\rho)\Big\{\psi^{(+)}(\rho)\Big[\theta(\rho_0-\rho)C^T J^{\nu'}(\rho) + \\ \theta(\rho-\rho_0)\Big(C^T J^{\nu'}(\rho_0) - I^{(-)\nu'}(\rho) + I^{(-)\nu'}(\rho_0) - S(-I^{(+)\nu'}(\rho) + I^{(+)\nu'}(\rho_0))\Big)\Big] \\ + \left[\theta(\rho_0-\rho)\psi^{(a)}(\rho)C + \theta(\rho-\rho_0)(\psi^{(-)}(\rho) - \psi^{(+)}(\rho)S)\right] I^{(+)\nu'}(\rho)\Big\}. \end{aligned} \tag{A4}$$

Finally, splitting the integration region into two and using Eq. (A2), we obtain

$$\begin{aligned} i\langle\nu'|\gamma G_E^+\gamma|\nu\rangle = \int_0^{\rho_0} d\rho\lambda^{\nu T}(\rho)\left[\psi^{(+)}(\rho)C^T J^{\nu'}(\rho) + \psi^{(a)}(\rho)CI^{(+)\nu'}(\rho)\right] \\ + \int_{\rho_0}^\infty d\rho\lambda^{\nu T}(\rho)\left\{\psi^{(+)}(\rho)\left[\bar{x}^{\nu'} - I^{(-)\nu'}(\rho)\right] + \psi^{(-)}(\rho)I^{(+)\nu'}(\rho)\right\}. \end{aligned} \tag{A5}$$

APPENDIX B: MATRIX GREEN'S FUNCTION

Consider the Matrix Green's function for the coupled equations in Eq. (19),

$$\frac{1}{2m_\rho}\frac{d^2}{d\rho^2}\psi_{\mu\mu'}(\rho) - \sum_{\mu''}[U_{\mu\mu''}(\rho) + (e_\mu - E)\delta_{\mu\mu''}]\psi_{\mu''\mu'}(\rho) = 0.$$

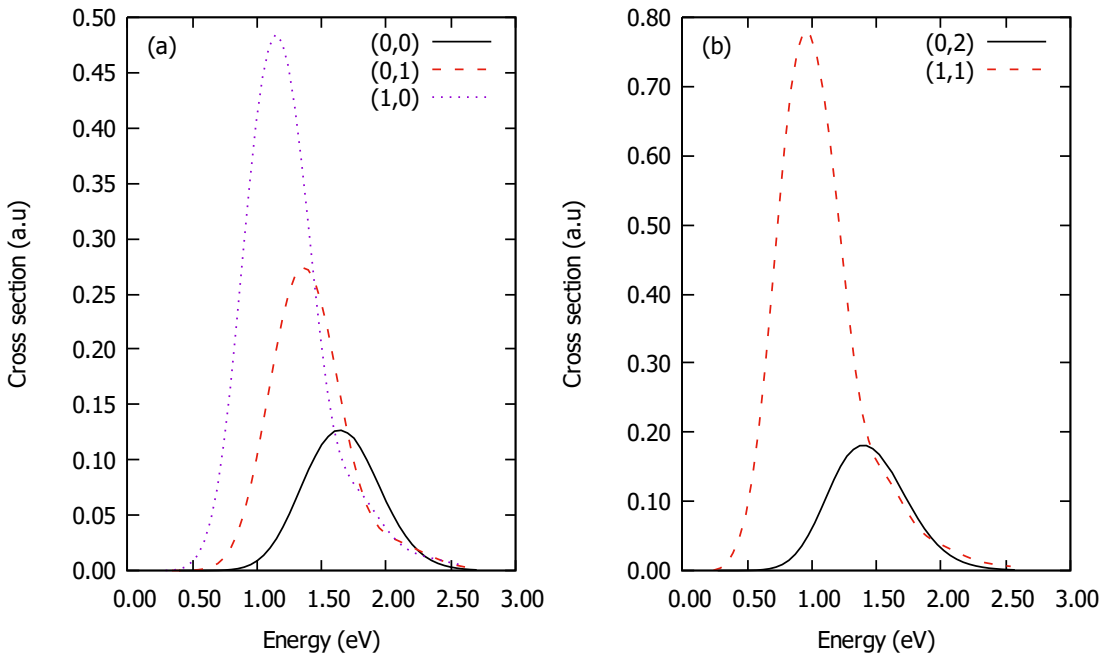

FIG. 11: DEA cross section when the target molecule is at specific excited state $\nu = (\nu_2, \nu_3)$, where ν_2 corresponds to umbrella vibrations of CF_3 fragment and ν_3 corresponds to the symmetric stretch of C-Cl. Panels (a) and (b) show the DEA cross sections when the target molecule is in the lowest excited states which are mixtures of umbrella and stretch vibrations.

The regular and irregular solutions of the homogeneous equation, $\psi^{(r)}_{\mu\mu'}$ and $\psi^{(+)}_{\mu\mu'}$, respectively, have the asymptotic boundary conditions

$$\psi^{(r)}_{\mu\mu'} \sim \psi^{(-)}_{\mu\mu'} - \psi^{(+)}_{\mu\mu''} S_{\mu''\mu'}, \quad \psi^{(\pm)}_{\mu\mu'} \sim \frac{\delta_{\mu\mu'}}{\sqrt{v_\mu}} e^{\pm iK\rho}$$

where $v_\mu = K_\mu/m_\rho$ and $K^2_\mu = 2m_\rho(E - e_\mu)$. In order for the Green's function to satisfy boundary conditions at 0 and ∞, it should have the following form

$$G_{\mu\mu'}(\rho,\rho') = \begin{cases} [\psi^{(r)}(\rho)A(\rho')]_{\mu\mu'} & \rho \le \rho' \\ [\psi^{(+)}(\rho)B(\rho')]_{\mu\mu'} & \rho \ge \rho' \end{cases} \tag{B1}$$

where the matrices A and B satisfy (from the conditions on the Green's function for equal arguments),

$$\psi^{(r)}(\rho')A(\rho') = \psi^{(+)}(\rho')B(\rho'), \tag{B2}$$

$$\left[\frac{d}{d\rho}\psi^{(+)}(\rho)\right]_{\rho=\rho'} B(\rho') - \left[\frac{d}{d\rho}\psi^{(r)}(\rho)\right]_{\rho=\rho'} A(\rho') = 2m_\rho \tag{B3}$$

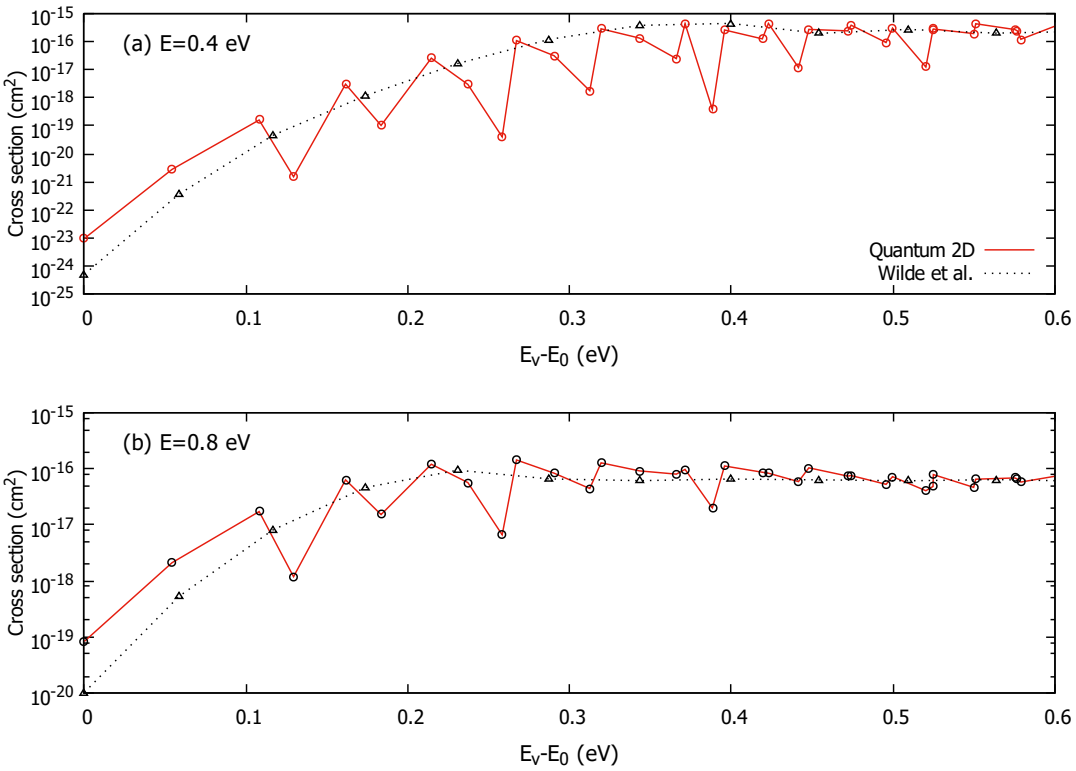

FIG. 12: Panel (a). DEA cross section as a function of vibrational energy when the incident electron energy is 0.4 eV. Present 2D quantum and semiclassical results are compared with the 1D quasiclassical approach as explained in [23]. Panel (b). Same as in Panel (a), but with an electron energy of 0.8 eV.

By multiplying Eq. (B2) with $[d\psi^{(+)T}/d\rho]_{\rho'}$ from the left, and Eq. (B3) with $\psi^{(+)T}(\rho')$ from the left, we have

$$\left[\left(\frac{d}{d\rho}\psi^{(+)T}\right)_{\rho'}\psi^{(r)} - \psi^{(+)T}\left(\frac{d}{d\rho}\psi^{(r)}\right)_{\rho'}\right]A + \left[\psi^{(+)T}\left(\frac{d}{d\rho}\psi^{(+)}\right)_{\rho'} - \left(\frac{d}{d\rho}\psi^{(+)T}\right)_{\rho'}\psi^{(+)}\right]B = 2m_\rho\psi^{(+)T} \tag{B4}$$

Both generalized Wronskians in the left-hand-side of Eq. (B4) are independent of ρ', therefore they can be calculated at the limit $\rho' \to \infty$ [67]. The first Wronskian gives a unit matrix multiplied by $2im_\rho$, and the second Wronskian is 0. Therefore

$$A = \frac{1}{i}\psi^{(+)T}(\rho') \tag{B5}$$

Similarly, multiplying Eq. Eq. (B2) by $[d\psi^{(r)T}/d\rho]_{\rho'}$ from the left, and Eq. (B3) by $\psi^{(+)T}(\rho')$ from the left, we have

$$B = \frac{1}{i}\psi^{(r)T}(\rho') \tag{B6}$$

Now, Eq. (B1) can be rewritten as

$$G(\rho,\rho') = \begin{cases} \frac{1}{i}\psi^{(r)}(\rho)\psi^{(+)T}(\rho') & \rho \le \rho' \\ \frac{1}{i}\psi^{(+)}(\rho)\psi^{(r)T}(\rho') & \rho \ge \rho' \end{cases} \tag{B7}$$

[1] A. Chutjian, A. Garscadden, and J. M. Wadehra, Phys. Rep. **264**, 393 (1996).

[2] L. G. Christophorou and J. K. Olthoff, *Fundamental Electron Interactions With Plasma Processing Gases* Kluwer Academic/Plenum Publ.: New York, 2004.

[3] I. I. Fabrikant, S. Eden, N. J. Mason and J. Fedor, Adv. At., Mol., Opt. Phys. **66** 545 (2017)

[4] O. Ingolfsson, in Low-Energy Electrons: Fundamentals and Applications Pan Stanford, Singapore 2019, p. 47.

[5] J. N. Bardsley, A. Herzenberg and F. Mandl, Proc. Phys. Soc. **89**, 321 (1966)

[6] I. I. Fabrikant, T. Leininger and F. X. Gadéa, J. Phys. B: At. Mol. Opt. Phys. **33**, 4575 (2000)

[7] I. I. Fabrikant, Phys. Rev. A **94**, 052707 (2016)

[8] S. T. Chourou and A. E. Orel, Phys. Rev. A **77**, 042709 (2008).

[9] S. T. Chourou and A. E. Orel, Phys. Rev. A **80**, 032709 (2009).

[10] S. T. Chourou, A. Larson, and A. E. Orel, Phys. Rev. A **92**, 022702 (2015).

[11] A. Orel and Å. Larson, Eur. Phys. J. D **74**, 15 (2020).

[12] Daniel J. Haxton, Zhiyong Zhang, H.-D. Meyer, T. N. Rescigno, and C. W. McCurdy, Phys. Rev. A **69**, 062714 (2004).

[13] Daniel J. Haxton, T. N. Rescigno, and C. W. McCurdy, Phys. Rev. A **75**, 012711 (2007).

[14] M. Tarana, P. Wielgus, S. Roszak and I. I. Fabrikant, Phys. Rev. A **79**, 052712 (2009)

[15] M. Tarana, K. Houfek, J. Horáček, and I. I. Fabrikant, Phys. Rev. A **84**, 052717 (2011)

[16] D. T. Birtwistle and A. Herzenberg, J. Phys. B **4**, 53 (1970).

[17] T. F. O'Malley, Phys. Rev. **150**, 14 (1966).

[18] J. N. Bardsley, A. Herzenberg, and F. Mandl, Proc. Phys. Soc. **89**, 305 (1966).

[19] J. N. Bardsley, J. Phys. B: At. Mol. Phys. **1**, 349 (1968)

[20] W. Domcke, Phys. Rep. **208**, 97 (1991).

[21] H. Hotop, M.-W. Ruf, M. Allan, and I. I. Fabrikant, Adv. At. Mol. Opt. Phys. **49**, 85 (2003).

[22] A. K. Kazansky, J. Phys. B **28**, 3987 (1995).

[23] R. S. Wilde, G. A. Gallup, and I. I. Fabrikant, J. Phys. B: At. Mol. Phys. **32**, 663 (1999).

[24] R. S. Wilde, G. A. Gallup, and I. I. Fabrikant, J. Phys. B: At. Mol. Phys. **33**, 5479 (2000).

[25] M. Braun, I. I. Fabrikant, M.-W. Ruf, H. Hotop, J. Phys. B: At. Mol. Phys. **40**, 659 (2007).

[26] M. Shapiro and R. Bersohn, J. Chem. Phys. **73**, 3810 (1980)

[27] G. Herzberg, *Molecular spectra and molecular structure*, Vol. 2 (Van Nostrand Reinhold, New York, 1945)

[28] S. Roszak, W. S. Koski, J. J. Kaufman and K. Balasubramanian, J. Chem. Phys. **106**, 7709 (1997).

[29] A. Gedanken and M. D. Rowe, Chem. Phys. Lett. **34**, 39 (1975).

[30] A. Mann and F. Linder, J. Phys. B **25**, 1621 (1992).

[31] C. W. Walter, B. G. Lindsay, K. A. Smith and F. B. Dunning, Chem. Phys. Lett. **154**, 409 (1989).

[32] A. Kalamarides, C. W. Walter, B. G. Lindsay, K. A. Smith, and F. B. Dunning, J. Chem. Phys. **91**, 4411 (1989).

[33] A. Kalamarides, R. W. Marawar, X. Ling, C. W. Walter, B. G. Lindsay, K. A. Smith, and F. B. Dunning, J. Chem. Phys. 92, 1672 (1990).

[34] R. Parthasarathy, C. D. Finch, J. Wolfgang, P. Nordlander, and F. B. Dunning, J. Chem. Phys. **109**, 8829 (1998).

[35] D. M. Pearl, P. D. Burrow, I. I. Fabrikant, and G. A. Gallup, J. Chem. Phys. **102**, 2737 (1995).

[36] A. Schramm, I. I. Fabrikant, J. M. Weber, E. Leber, M.-W. Ruf, H. Hotop, J. Phys. B **32**, 2153 (1999).

[37] T. Beyer, B. M. Nestmann, and S. D. Peyerimhoff, J. Phys. B **34**, 3703 (2001).

[38] I. Hahndorf, E. Illenberger, L. Lehr and J. Manz, Chem. Phys. Lett., **231**, 460 (1994)

[39] S. Marienfeld, T. Sunagawa, I. I. Fabrikant, M. Braun, M.-W. Ruf, and H. Hotop, J. Chem. Phys. **124**, 154316 (2006)

[40] S. Goursaud, M. Sizun, and F. Fiquet-Fayard, J. Chem. Phys. **65**, 5453 (1976).

[41] L. Lehr and W. H. Miller, Chem. Phys. Lett., **250**, 515 (1996)

[42] L. Lehr, J. Manz, and W. H. Miller, Chem. Phys. **214**, 301 (1997).

[43] I. I. Fabrikant, Phys. Rev. A **43**, 3478 (1991).

[44] I. I. Fabrikant, Phys. Rev. A **94**, 052707 (2016).

[45] D. J. Haxton, C. W. McCurdy, and T. N. Rescigno, Phys. Rev. A **73**, 062724 (2006).

[46] M. LeDourneuf, B. I. Schneider and P. G. Burke, J. Phys. B At. Mol. Phys. **12**, L365 (1979).

[47] A. M. Lane and R. G. Thomas, Rev. Mod. Phys. **30**, 257 (1958)

[48] I. I. Fabrikant, Comments on At. Mol. Phys. **24**, 37 (1990).

[49] R. K. Nesbet, Phys. Rev. A **19**, 551 (1979).

[50] L. F. Canto and M. S. Hussein, *Scatering theory of molecules, atoms and nuclei*(World Scientific, Singapore, 2013)

[51] S. A. Kalin and A. K. Kazansky, J. Phys. B **23**, 4377 (1990).

[52] J. H. Van Vleck, Proc. Natl. Acad. Sci. U.S. **14**, 178 (1928).

[53] M. C. Gutzwiller, J. Math. Phys. **11**, 1791 (1970).

[54] M. C. Gutzwiller, J. Math. Phys. **8**, 1979 (1967).

[55] W. H. Miller, J. Chem. Phys. **95**, 9428 (1991).

[56] E. J. Heller, J. Chem. Phys. **94**, 2723 (1991).

[57] W. H. Miller, J. Chem. Phys. A **13**, 105 (2001)

[58] K. Scanlon, I. Suzuki, and J. Overend, J. Chem. Phys. **74**, 3735 (1981).

[59] M. Suto and N. Washida, J. Chem. Phys. **78**, 1012 (1983).

[60] A. K. Kazansky and I. S. Yelets, J. Phys. B: At. Mol. Phys. **17**, 4767 (1984).

[61] I. S. Yelets and A. K. Kazansky, JETP **55**, 258 (1982).

[62] I. I. Fabrikant, Z. Phys. D **3**, 401 (1986).

[63] M. S. Child, *Semiclassical mechanics with molecular applications*, Second edition (Oxford University Press, United Kingdom, 2014)

[64] T. N. Rescigno and C. W. McCurdy, Phys. Rev. A **62**, 032706 (2000).

[65] A. L. Kaledin and W. H. Miller, J. Chem. Phys. **118**, 7174 (2003)

[66] H. Wang, D. E. Manolopoulos and W. H. Miller, J. Chem. Phys. **115**, 6317 (2001)

[67] G. A. Gallup, Y. Xu, and I. I. Fabrikant, Phys. Rev. A **57**, 2596 (1998).